



0895-6111(94)00041-7

## CT VOLUMETRIC DATA-BASED LEFT VENTRICLE MOTION ESTIMATION: AN INTEGRATED APPROACH

Chang Wen Chen,<sup>\*1</sup> Jiebo Luo,<sup>\*</sup> Kevin J. Parker,<sup>\*</sup> and Thomas S. Huang<sup>†</sup><sup>\*</sup>Department of Electrical Engineering, University of Rochester, Rochester, NY 14627-0231<sup>†</sup>Beckman Institute and Coordinate Science Lab, University of Illinois at Urbana-Champaign, Urbana, IL 61801

(Received 9 May 1994)

**Abstract**—This paper describes a novel approach to left ventricle motion analysis via the integration of image segmentation with shape deformation analysis using computerized tomography (CT) volumetric image data. This approach is different from traditional image analysis scenario in which the image segmentation and shape analysis were considered separately. The advantage of integrating the image segmentation with the shape analysis lies in the fact that the shape characteristics of the object can be used as effective constraints in the process of segmentation while original image data can be made useful along with the segmentation results in the process of shape analysis. In the case of left ventricle motion estimation, such an integration can be applied to obtain the estimation results that are consistent with both given image data and a priori shape knowledge. The initial segmentation of the images is obtained through adaptive *K*-mean classification and the region-of-interest is then identified based on the initial segmentation. The shape analysis is accomplished through fitting the boundary points of the region-of-interest to the surface modeling primitives. These two processes are integrated through the feedforward and feedback channels so that the surface fitting is constrained by the confidence measures of the boundary points and segmentation refinement is guided by the result of surface modeling. Global motion parameters are obtained by comparing the parameters of the fitted surface model at consecutive time instances. The segmentation and shape analysis results obtained show that the integrated approach is capable of providing promising improvement over traditional approaches.

**Key Words:** Cardiac motion analysis; Cardiac image processing; Image segmentation; Nonrigid motion estimation; Shape analysis; Integration

### 1 INTRODUCTION

Left ventricle motion analysis from image sequences has received considerable attentions for the past few years. The problem is very challenging since the heart is a nonrigid object and the description of its motion over a cardiac cycle usually requires the displacement information of each localized material element. However, it is an important research topic in the area of biomedical engineering because of its noninvasive nature in assessing the cardiac dynamic behavior. Such assessment can be an invaluable tool in diagnosis of heart disease, monitoring of cardiac therapy, and other clinical and research applications. The left ventricle as a whole is a nonrigid object and its shape changes over the cardiac cycle. The shape change of the left ventricle is due to the global and local deformations during the pumping of the heart. Logically, deformation modeling of the left ventricle, global or local, can be realized by surface modeling if we are able to incorporate the deformation parameters into the surface modeling

primitives. In the earlier study of left ventricle dynamics based on surface modeling, simple surface models such as ellipsoid and cylinder have been assumed. These simplified surface primitives are very crude representations based on a priori knowledge of the left ventricle shape. The analysis based on these simple surface primitives provide only limited qualitative measure of the left ventricle dynamics. The lack of ability to incorporate deformation parameters into these simple models makes them inapplicable to quantitative analysis of typical deformations such as tapered shape and non-uniform dilation. We proposed a class of three-dimensional (3D) shape modeling primitives called superquadrics to include the deformations that were unable to be incorporated into the simple models. The superquadric shape modeling has been successfully applied to motion and deformation analysis of left ventricle (1, 2).

To analyze the shape of an object based on a given image or a stack of images, the extraction of object shape is usually accomplished through the segmentation process. A subsequent analysis of the object shape is then based on the results of such segmentation, or

<sup>1</sup> To whom correspondence should be addressed.

shape extraction. Traditionally, the segmentation is based only on image features, such as gray level, texture, and color without utilizing the shape properties of the object, while the shape analysis is based on the final result of segmentation without regard to the confidence measure of the shape extraction. It is evident that such separated processing and analysis, at least, have not completely made use of all the available information. Due to the lack of interaction between segmentation and shape analysis, many existing approaches have produced object boundary inconsistent with a priori knowledge, or shape parameters inconsistent with the given image data. In biomedical applications, we look for certain structures in the given images and therefore the shape information is known to us to a certain degree. Hence, the shape information should be used to guide the segmentation process to overcome the difficulty of segmentation using noisy image data and to refine the crude segmentation through feedback. On the other hand, the estimated boundary points based on the segmentation are often ambiguous due to the poor contrast of the discontinuities. The degree of such ambiguity can be a meaningful confidence measure associated with each extracted boundary point and should be used in the fitting of shape modeling primitives. Without the confidence measure, the surface parameter estimation would be derived from all the boundary points with equal weights. This implies that all the boundary points have equal strength which is generally not true.

Over the years, there have been some researchers who have attempted to develop segmentation algorithms suited for certain class of boundary extraction. Their approaches can be generally divided into two major categories: optimization in parameter space and optimization in image space. In the case of boundary finding through the optimization in parameter space, a class of parameterized templates are used to model the objects. Examples of this type of approaches include the rubber masks proposed by Widrow (3), eye template and mouth template described by Yuille, Cohen, and Halliman (4), and deformable hand models developed by Grenander, Chow, and Keenan (5). All these approaches have been implemented through fitting the model to the image data by searching the parameter space for the best fit. In the case of boundary finding through the optimization in image space, the measure of fit is represented by certain image related quantities. Some of these approaches use a flexible bead chain to represent the boundary points and make them attracted to the pixels with certain image statistical properties (6, 7). Among those image space based approaches, an elegant approach proposed by Kass, Witkin, and Terzopoulos (8) uses the boundary model primitives

called snakes to form an energy minimization problem. The snakes are attracted to boundary by external and internal forces. The internal forces are composed of mainly the smoothness constraints of the snakes, while the external forces are the image features such as edges and lines. As opposed to the parameter space based boundary representation, the image space based representation and optimization are difficult to incorporate the a priori shape information, especially those algebraic properties of the surface modeling primitives other than the smoothness.

We propose a novel approach to left ventricle motion and deformation analysis through the integration of image segmentation and shape analysis. Our proposed approach is different from both types of traditional segmentation approaches in that we consider the optimization in both image and parameter spaces. The advantage of this approach over existing approaches lies in the fact that the interactions between the image segmentation and subsequent shape analysis are exploited so that all the available information can be made use of in either image segmentation or shape analysis. Since both image segmentation and shape analysis have been traditionally formulated as optimization problems, the interactions between these two processes can therefore be used to form additional constraints in each of the original optimization processes. These constrained optimizations in image segmentation and shape analysis constitute an integrated approach to image analysis and provide each process a dimension for major improvement. However, there has not been enough effort made along this direction of research. This paper is intended to serve as an initiative to promote the integration of image segmentation with the shape analysis through the estimation of left ventricle motion using CT volumetric image data.

In this research, we are given a sequence of 16 CT volumetric images, each with the dimension  $90 \times 90 \times 95$ . Our earlier studies (2) have concentrated on the shape analysis using digital volumes obtained through manual outlining of original images. The goal of this research is to develop a systematic approach for cardiac motion analysis such that the original gray level volumetric images are directly used without time consuming manual outlining by skilled operators. We propose to integrate multiple processes involved in the cardiac image analysis utilizing the original gray level images as well as a priori shape knowledge of the left ventricle. The processes of image segmentation, region-of-interest (ROI) identification and subsequent shape analysis are effectively integrated to produce better results than the results produced by traditional approaches in which these processes are separately implemented. To achieve this goal, a key step of the

research is to identify the interdependent relations between these optimization processes, since these relations serve as the channels for mutual feedback and can be used to form well defined constrained optimizations in the process of integration. The research presented here is motivated by surface modeling based left ventricle motion and deformation analysis using CT volumetric image data. However, this integrated approach can be applied to a wide variety of other image analysis tasks when the shape information of the object is available. Some other forms of surface modeling primitives can be used to suit the specific class of object shape under consideration.

Section 2 describes the acquisition of CT volumetric images and the appearance of cardiac anatomy in such a volume. The knowledge of the cardiac anatomy and its appearance is used in designing the image segmentation algorithm. Section 3 presents the overall scheme of the integrated approach and identifies the interdependence between the process of image segmentation and the process of shape analysis. Section 4 describes the implementation details of image segmentation and shape analysis, as well as the feedforward and feedback channels. Section 5 presents the results obtained based on this integrated approach and Section 6 concludes this paper with summary of this research and discussions of future research plans.

## 2 DATA ACQUISITION AND LEFT VENTRICLE ANATOMY

Our CT volumetric data sets are obtained from the Dynamic Spatial Reconstructor (DSR), the unique ultra-fast multislice scanning CT system built and managed by the Mayo Foundation (9). Compared to commercially available Picker Fastrac, or Imatron scanners, the DSR scanner has functional flexibility in that the spatial, temporal, and contrast resolution can be adjusted to favor one aspect of resolution over the other. This flexibility facilitates basic research applications.

According to Dr. Ritman and his colleagues (10, 11), the DSR synchronously scans multiple, parallel, transaxial sections within  $\frac{1}{100}$  s. These scans are repeated 60 times per second. Up to 120 images of transaxial sections were reconstructed for each  $\frac{1}{60}$  s scan sequence, and post scan manipulation and interpolation of the reconstructed images were used to generate cubic voxels of such volumetric image sequences. With such rapid, extensive data collection, high-resolution volumetric images, largely free of motion blur, can be generated for moving organs, such as the heart. In a typical DSR experiment, 16 volumes are reconstructed within a cardiac cycle, with each volume rep-



Fig. 1. A few typical cross sections of the original DSR data.

resenting one time instant. Each reconstructed volumetric image usually contains roughly  $120 \times 128 \times 128$  slices, however, this research is based on a sequence of 16 volumes each contains  $95 \times 90 \times 90$  slices. Each slice of a reconstructed volume represents an approximately 0.9 mm thick transverse cross section of the scanned anatomy, and each of the volumetric elements, or voxels, represents an  $(0.9 \text{ mm})^3$  cube of tissue. To bring out the left ventricle chamber as a bright object, a Roentgen contrast agent is injected into the right atrium several seconds prior to the scanning of the heart. A few cross sections of the original DSR data are presented in Fig. 1.

In a typical volume of such images, the left ventricle is included in a high intensity region which would also include the left atrial chamber and aorta. Although there are valves separating the left ventricle chamber from the left atrial chamber and aorta, the valves of canine heart, which has been used in this basic research rather than the human heart, are only of the order of 1 mm thick and their visibility in the volume is diminished by the partial volume effect and the resolution limitation of DSR scanner (12). Furthermore, the valves open and close alternatively during a cardiac cycle so that whether or not they appear in an acquired image would also depend on the timing of the image acquisition. Therefore, the left ventricle often appears connected with the left atrial chamber and aorta in the acquired volumetric images.

Overall, the intensity of the left ventricle is much brighter than the myocardium. However, the intensity distribution of the left ventricle chamber is not uniform due to the uneven distribution of the contrast agent. The nonuniform distribution of the contrast agent is difficult to model and compensate, and therefore requires the image segmentation algorithm to be adaptive

to local properties of the intensity distribution. In addition to the nonuniform distribution of contrast agent, the noise from the errors in scanning and volume reconstruction causes the blurring of the structural borders and hence introduces the ambiguity in boundary classifications. According to Dr. Higgins (11), the left ventricle chamber appeared in the CT volumetric images is a large, bright, smooth, solid region, varying in size and shape over time, approximately attached to the left atrial chamber and aorta through the valves, and separated from the myocardium by a strong, but blurred and noisy, interface.

This general image model of the left ventricle is used in the design of the clustering algorithm for the image segmentation. We design a robust image segmentation algorithm using the image model of the left ventricle such that it is adaptive to spatial-varying image intensity of the left ventricle caused by the nonuniform distribution of the contrast agent. This image model of left ventricle will also be used to devise an ROI identification algorithm using various morphological operations to produce the digital volumes containing only the left ventricle chamber. The blurred and noisy boundary between left ventricle chamber and myocardium caused by errors in scanning and reconstruction is used to compute the segmentation confidence measures used in the implementation of the shape analysis algorithms to enforce the data consistency constraint. The shape information of the left ventricle, which generally can not be inferred from the image, is used as the guidance for the segmentation refinement so that the final segmentation is compatible with the surface modeling primitives derived from a priori shape knowledge. The overall scheme of the integration for a general purpose image analysis task is described in Section 3. The detail of how multiple sources of information are utilized in implementing an integrated algorithm for left ventricle motion analysis is given in Section 4.

### 3 OVERVIEW OF THE INTEGRATED APPROACH

The overall block diagram of the integration is presented in Fig. 2. The image segmentation process includes the adaptive *K*-mean clustering and ROI identification. The shape analysis process includes the construction of the object centered coordinate system and the fitting of shape modeling primitives. The feedforward channel from the segmentation to the shape analysis is formed through the application of confidence measures derived from the original image data to the fitting of the boundary points to shape modeling primitives. The feedback channel from shape analysis to

segmentation is formed through the masking of the region of adjustment in the given images followed by the necessary procedures for shape knowledge based segmentation refinement.

The block diagram in Fig. 2 represents the overall scheme of integration for a general image analysis task based on surface modeling. For each specific problem, the implementation of the algorithms within the integrated frame will be different from one to another. In general, the original image data sets are first passed through an adaptive *K*-mean clustering algorithm to obtain an initial segmentation. The knowledge of the object shape, such as the anatomy of biomedical structures, is applied to identify the ROI. The ROI identification process can be implemented, in many cases, by the morphological operations on the segmented regions. The boundary of this ROI is then extracted and the confidence measure of each boundary point is computed. The confidence measure of a boundary point includes the neighborhood information such as magnitude of the gradient and the difference between its grey-level value and class mean. The subsequent construction of the object centered coordinate system is usually the first step in shape analysis in order to align the position and orientation of the region-of-interest for normalized deformation analysis. The confidence measures weighted fitting of the normalized boundary points to surface modeling primitives provides a parameterized characterization of shape deformations. After the surface fitting, the energy functions of the errors in both image segmentation and surface fitting are combined to compute the total energy function of the system. If the energy of the system has not reached the minimum, the feedback channel is opened for segmentation refinement. Then, the fitted surface is projected back to the original image space to form masked regions composed of inconsistently classified pixels. Within these masked regions, the grey level value of their pixels is updated according to the nature of the classification inconsistency. A stochastic updating scheme is developed to ensure the randomness of the pixel gray level updating considering that the images have in fact been corrupted by various types of noise. Upon the completion of the pixel value adjustment, a new cycle of image segmentation and shape analysis is performed, beginning with the adaptive *K*-mean clustering for segmentation refinement. Such cycle of iteration is continued until the system energy reaches the minimum.

It can be seen from the block diagram that an output of this system is the parameterized surface representing the object under consideration. Traditional segmentation algorithms usually consider the segmented regions as their final results without concerning

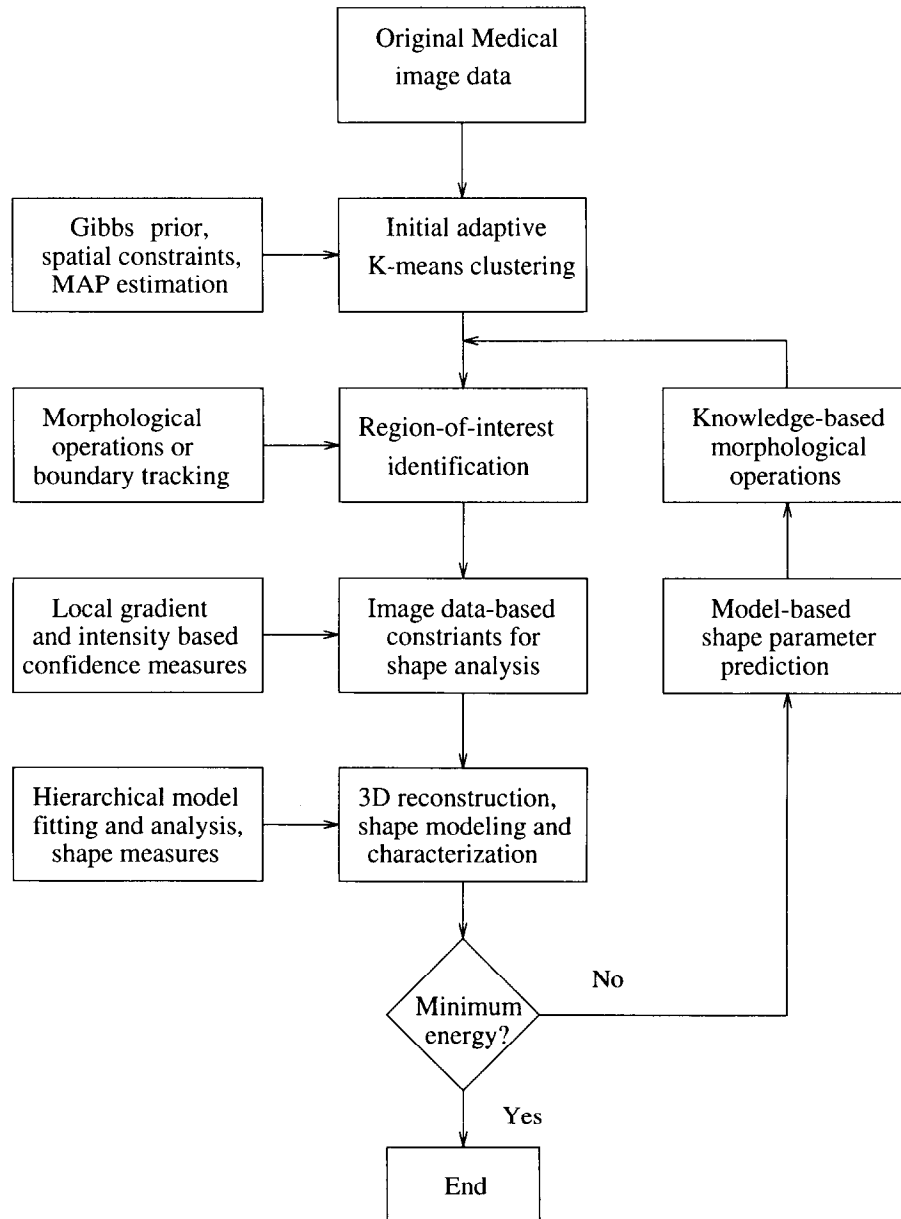


Fig. 2. Block diagram of the integrated approach.

the nature of the subsequent analysis based on the segmented results. For general image analysis tasks, we usually do not stop at the stage of segmentation, instead, we treat the segmentation as an effective way of representing the image information for subsequent segmentation based further analysis. The segmentation of a given image serves only as an intermediate result, and in fact, as the input to the shape analysis process. Hence, the clustering and segmentation of structure-of-interest based on the original image data should be an integral part of the overall image analysis system. An overall optimal solutions can only be obtained

through integrating the segmentation with other components within such a system. The feedforward channel in this integrated approach is designed to enforce the constraints of data consistency on the surface analysis process. These constraints are imposed in the form of weighted surface fitting through the applications of confidence measures derived from the original images data. Such weighted surface fitting is able to integrate the segmentation results with the original image data to achieve a data consistent results. On the other hand, the a priori shape knowledge of the object under consideration can be very useful in the process of segmen-

tation in order to determine what type of structure one should look for. Unfortunately, such a priori knowledge have not been used in existing segmentation algorithms. Many segmentation algorithms have thus produced segmented regions inconsistent with a priori knowledge. The feedback channel in this proposed approach serves as a guidance for the refinement of image segmentation so that the segmented region is compatible with a priori shape knowledge of a given object. Without doubt, this feedback of shape information would provide an opportunity for the shape analysis process to integrate with the segmentation process so that both the image data and shape information are used to generate accurately segmented regions from the noisy images. Through integration, the linkage between the process of image segmentation and the process of shape analysis has been enforced in a dual directional fashion.

#### 4 IMPLEMENTATION OF THE INTEGRATED APPROACH

We have presented, in Section 3, the overall description of the integrated approach. The system of integration consists of three major components: image segmentation, shape analysis, and their interactions. Such integrated scheme can be applied to many image analysis tasks based on parameterized surface modeling. However, the implementation of the integration scheme for each specific problem is different from one to another because different objects often have distinct shape characteristics. These shape characteristics determine how the segmentation and ROI identification should be done and what type of surface modeling primitives should be employed. In the case of left ventricle motion analysis based on surface modeling, the algorithms for initial segmentation and ROI identification are designed based on a priori information of the heart anatomy and the appearance of left ventricle in the given image. The surface modeling primitives are also derived from a priori shape knowledge of the left ventricle widely used in cardiac research. In the following, we discuss in detail the implementation of the algorithms in this integrated approach for left ventricle motion estimation.

##### 4.1 Segmentation and ROI identification algorithms

For many image analysis applications, we are often interested in only a single region or a cluster of regions that are the projection of an object-of-interest in a given image. This is particularly true for biomedical applications when we look for certain structures from a given image or a set of image data. The first step in such image analysis applications is to identify

the region-of-interest from the image data. In the case of left ventricle motion analysis, we are given a sequence of volumetric image data representing the dynamics of the heart. The left ventricle can be identified from the given image sequence since it is contained within a bright region produced by the contrast agent. However, as we have pointed out in Section 2, the design of the segmentation and ROI identification algorithms is challenging since the algorithms need to extract the left ventricle chamber from the given images having nonuniform intensity distribution within the region-of-interest, blurred and noisy interface between left ventricle and myocardium, and ambiguous separation between left ventricle and left atrium and aorta. After the successful extraction of the left ventricle chamber from a given volume of image data, the boundary of the extracted region is used for the subsequent process of shape analysis.

*4.1.1 The adaptive K-mean segmentation.* Image segmentation is an important, yet challenging problem in image processing and image analysis. There have been numerous algorithms developed over the years. Depending on the goal of the research, the algorithms of image segmentation range from generating binary representation from a gray level image to tracking of time-varying regions in a given image. However, there is one thing in common for all the segmentation algorithms, that is, they all seek to develop an accurate and compact representation of the information contained in the images. The representation of the extracted information is usually critical for further analysis and processing. In the case of extracting region-of-interest from the images, many thresholding based approach have been developed. The thresholding based approaches generally classify each image element as either a member of the region-of-interest or a non-member of that region. The major drawback of these thresholding based approaches is the binary nature of the clustering that usually produces inaccurate classification of regions since natural and biomedical images are often composed of more than two clusters of image elements representing corresponding types of different objects or structures. In particular, when the image segmentation or region extraction techniques are applied to biomedical images with known number of multiple clusters, an algorithm better than the thresholding based approach can be designed. This multi-cluster classification of images is known as the *K*-mean image segmentation and can be applied to many biomedical image analysis problems since the value of *K* can be determined a priori for images of particular parts of human anatomy.

The traditional *K*-mean image segmentation algo-

gorithms and their variations classify the pixels in an image into clusters based only on their intensity. Each cluster of pixels is characterized by a constant intensity and is free of any spatial constraints. In practice, the images are noisy version of the reflected density function, and the image intensity of same cluster may change over the spatial domain due to some physical limitations of the imaging system. Furthermore, certain spatial constraints are needed since a pixel tends to belong to the same class as most of its neighbors unless it is on the boundary of sharp region transition. Our adaptive  $K$ -mean segmentation algorithm is based on the approach proposed in (13) in which both spatial constraints and varying intensity functions are included in the adaptive process. We have extended that approach to include an additional constraint that the estimated variance of each cluster is adaptively updated in the process of classification. Essentially, the adaptive  $K$ -mean segmentation algorithm makes use of spatial information by assuming that the distribution in regions is described by a Gibbs random field with its parameters representing the size and shape of the region. A Maximum A Posteriori (MAP) algorithm is used to characterize the spatial varying intensity change of the left ventricle chamber caused by inhomogeneity of contrast agent distribution in the CT images.

It has been shown that (13, 14) images can be modeled as a Gibbs random field and the segmentation can be accomplished through MAP estimation techniques. According to Bayes' rule, the posterior probability can be expressed as:

$$p(x|y) \propto p(y|x)p(x), \quad (1)$$

where  $p(x)$  is the a priori probability of the segmentation, and  $p(y|x)$  represents the conditional probability of the image data given the segmentation. The Gibbs random field can be characterized by a neighborhood system and a potential function. An image segmentation is accomplished by assigning labels to each pixel in the given image. A label  $x_s = i$  implies that the pixel  $s$  belongs to the  $i$ -th class of the  $K$  classes. Therefore, we have:

$$p(x_s|x_t, \forall t \neq s) = p(x_s|x_t, t \in N_s), \quad (2)$$

where  $N_s$  represents the defined neighborhood for pixel  $s$ . Associated with each neighborhood system are cliques and their potentials. A clique is a set of sites where all elements are neighbors. A Gibbs distribution can then be defined as:

$$p(x) \propto \exp\left\{-\sum_C V_C(x)\right\}, \quad (3)$$

where  $V_C$  is a certain clique potential function for clique  $C$ . If we model the conditional density as a

Gaussian process, then the overall probability function will be:

$$p(x|y) \propto \exp\left\{-\sum_s \frac{1}{2\sigma_s^2} (y_s - \mu_s)^2 - \sum_C V_C(x)\right\}. \quad (4)$$

where  $\mu_s$  and  $\sigma_s$  are the class mean and variance at pixel location  $s$ . MAP estimation can be implemented based on Equation 4 using optimization techniques. In this process,  $\mu_s$  and  $\sigma_s$  are adaptively estimated and updated so that the segmentation algorithm can be applied to images of spatial varying intensity associated with the left ventricle. This adaptive clustering algorithm is applied to obtain four regions with the brightest region corresponding to left ventricle chamber.

*4.1.2 ROI identification.* For many biomedical applications, we know in advance the approximate size and shape of the object we are looking for from the images. Due to the errors in scanning and reconstruction of the original images, the results from image segmentation using adaptive  $K$ -mean clustering may still contain small regions that have been mis-classified. The knowledge of the object shape and size can now be used to eliminate any region that are not compatible with the a priori knowledge. In the case of left ventricle chamber extraction, after the completion of adaptive  $K$ -mean segmentation, all the pixels that have been segmented into the brightest region are first considered as potentially belonging to the left ventricle while the rest of pixels are considered as not belonging to the left ventricle. This binary re-classification is based on the results of  $K$ -mean segmentation, however, it is necessary to use multi-cluster segmentation ( $K = 4$ ) instead of thresholding in the process of initial segmentation. Notice that the segmentation of left ventricle chamber would be incorrect if we use thresholding ( $K = 2$ ) directly in the process of initial segmentation since the given images indeed consists of four representative regions corresponding to four types of biomedical structures that produce different densities in the image.

Based on the description presented in Section 2 on how the left ventricle chamber would appear in a given image, the ROI is assumed to be one single bright region. Hence, the small isolated bright regions should either be merged with the main region if they are in the neighborhood of the ROI, or be labeled as non-ROI according to model of the appearance of the left ventricle. To achieve these goals, we have designed a combination of digital morphological operations on the initial segmentation results and obtained the desired results. The resultant single bright region represents the connected volume consisting of the left ventricle, left atrium and aorta. The morphological operations

used to obtain such volume include opening, ( $O$ ) and closing, ( $C$ ) which are in turn defined by basic morphological operations, such as dilation, ( $D$ ) and erosion, ( $E$ ) (15). The opening and closing are defined as:

$$O(A, B) = D[E(A, B), B] \quad (5)$$

$$C(A, B) = E[D(A, -B), -B] \quad (6)$$

where  $A$  is the image and  $B$  is the operation element and  $-B$  denotes the reflection of  $B$  with respect to its origin.

We then begin to eliminate the left atrium and aorta from the resultant volume after completion of these morphological operations, since the further analysis of left ventricle dynamics would require the given volume to consist only the left ventricle. There has been no existing method of automatically identifying the separations between the left ventricle chamber and the left atrium and aorta in a given CT images. Higgins and his colleagues have recently worked towards an automatic segmentation of left ventricle from these volumetric images (11, 16), however, the separation of left ventricle from left atrium and aorta is accomplished either manually in advance or interactively by a skilled operator. We proposed to use predictive morphological operations to identify the left ventricle chamber from this composite region. The basic morphological operation is erosion, though, the position and area of the seed region are obtained from the predictions computed from previous cross sections according to the shape modeling primitives. We have achieved promising results with these knowledge-based morphological operations. The detail of such predictive morphological operations is described in (17). The resultant volume after predictive morphological operations is considered as the segmented left ventricle chamber. The boundary of this region is then extracted using simple manipulation on the binary data and will be used as the input to the shape analysis algorithms.

#### 4.2 The shape analysis algorithms

Given the extracted 3D structures from the volumetric images, the next step in biomedical image analysis is to infer physiology or pathology related information from such structures. Simple calculation of volume measurement from the extracted structure has often been adopted since the computation of more complicated measures usually requires better understanding of the given object or structure. However, for many biomedical structures, the shape characterization has important clinical and research applications beyond what simple volume measure could provide since

many physiological properties of a given structure are more closely related to shape deformations in either spatial or temporal domains. Shape analysis of biomedical structures usually provides more detailed and localized information than the volume analysis which generally provides only global measures. In particular, the left ventricle is considered as a deformable object that changes its shape continuously over the cardiac cycle. The shape characterization of left ventricle chamber is therefore a vital component of the cardiac image analysis.

The shape modeling based algorithms have been successfully applied to motion and deformation estimation of various deformable objects (1, 18, 19). It is true that the 3D dynamic surface models employed in these approaches are different from one application to another. However, the implementation of the shape modeling based approaches are generally accomplished by surface fitting. The motion and deformation parameters of the object are then usually obtained by comparing the implicit shape parameters of the fitted surface at two consecutive time instants. Among these shape modeling based approaches, the hierarchical scheme of modeling and estimation of surface motion and deformation has led to a computationally efficient implementations (18). Our shape modeling and analysis algorithms for left ventricle motion and deformation estimation are hence based on the principles of hierarchical modeling and estimation.

In our hierarchical modeling and estimation based approach, the motion and deformation parameters are obtained by comparing the corresponding parameterized surfaces. Logically, such comparisons of parameterized surfaces can only be made with the assumption that the representations of the surfaces are with respect to the same reference coordinate system. Therefore, the first step in the process of shape analysis is to construct an object centered coordinate system and transform all the boundary data points to this coordinate system before the next step of fitting of the shape modeling primitives is undertaken. The procedures of coordinate system construction and shape modeling primitives fitting are repeated for every volume in a given image sequence. The details of how the motion and deformation parameters are computed from the fitted parameterized surfaces are described in (1).

*4.2.1 Object centered coordinate system.* The establishment of the object centered coordinate system is necessary for the surface modeling based nonrigid motion analysis. In the hierarchical scheme of modeling and estimation of left ventricle motion and deformation, the origin and orientation of the this coordinate system is computed from the estimated long axis of

the left ventricle extracted from the given discretized boundary of the ROI. In addition, the curvature of the estimated long axis is also used to represent the overall bending deformation of the left ventricle under the assumption that the left ventricle is having linear bending deformation during the cardiac cycle.

It has been shown that (20, 21) the center-of-contraction of the left ventricle surface can be used to represent the estimated origin of the object centered coordinate system. The computation of the center-of-contraction is usually accomplished through least square estimation if one is given the corresponding surface points at two consecutive time instants. When no such correspondence but a dense cluster of surface points are given, a good approximation of the center-of-contraction is the center-of-gravity of the given surface points (21). We have also shown in (21) that this center-of-gravity is equal to the weighted centroid of all cross section centroids in a given volume. The weight of each cross section is equal to the relative number of boundary points within the given cross section. Although the center-of-gravity can be computed directly from all the boundary points, the computation of center-of-gravity from cross section centroids can be conveniently incorporated with the construction of the long axis which is used to estimate the orientation of the object centered coordinate system as well as the bending deformation of the left ventricle chamber.

In the case of left ventricle, the motion of its long axis is a clear indication of its position and orientation changes. Generally, the long axis of the left ventricle is defined as a curved line connecting the center of the base and the apex of the left ventricle. We shall assume that this curved long axis lies approximately on a plane whose motion is driven mostly by the overall position and orientation change of the left ventricle (21). Such assumption has been implicitly used in many previous studies of left ventricle dynamics since the long axis is often assumed to be only a straight line (22). In the case of CT volumetric data, the discrete representation of the long axis can be approximated by the centroids of cross sections, assuming that these cross sections are obtained transversely. Then, upon the extraction of cross section centroids, the plane that the long axis lies can be constructed through estimating a best-of-fit plane based on the extracted centroids. This plane is determined from a  $3 \times 3$  scattering matrix computed from the given cross section centroids such that the normal of this plane coincides with the eigenvector that corresponds to the smallest eigenvalue of the scattering matrix. Since the scattering matrix is symmetric and positive definite, its three eigenvectors are ordered according to the error-of-fit and are mutually orthogonal. The order of these eigenvectors is assumed unchanged

since the twisting deformation of the left ventricle is generally small compared with other forms of global motion and deformation (20). Therefore, these ordered eigenvectors can be used to represent the orientation of the object centered coordinate system. After the determination of the object centered coordinate system, we follow the procedures described in (21) to compute the global rigid motion and bending deformations. Essentially, the global translation is the difference between the origins of two object centered coordinate systems, and the global rotation is the orientation change of these two coordinate systems. In matrix form, the global translation and rotation parameters of the left ventricle can be written as:

$$T = \begin{bmatrix} x'_m \\ y'_m \\ z'_m \end{bmatrix} - \begin{bmatrix} x_m \\ y_m \\ z_m \end{bmatrix} \quad (7)$$

$$R = [\mathbf{e}'_1 \ \mathbf{e}'_2 \ \mathbf{e}'_3][\mathbf{e}_1 \ \mathbf{e}_2 \ \mathbf{e}_3]^T \quad (8)$$

where  $(x_m, y_m, z_m)$  and  $(x'_m, y'_m, z'_m)$  are the centroids, and  $\mathbf{e}_1, \mathbf{e}_2, \mathbf{e}_3$  and  $\mathbf{e}'_1, \mathbf{e}'_2, \mathbf{e}'_3$  are the eigenvectors of the scattering matrices at two consecutive time instants. The bending deformation parameters are obtained through fitting the cross section centroids to an arc since linear bending is assumed. For linear bending, a straight line becomes an arc with radius  $R$ , and the bending rate is equal to  $\frac{1}{R}$ . These estimated motion and deformation parameters are used to transform the extracted discretized version of the left ventricle boundary to an object centered coordinate system in which the surface fitting and parameterization can be implemented coherently.

*4.2.2 Fitting of surface modeling primitives.* Superquadrics are used in this research as the surface modeling primitives for the left ventricle. It is a parameterized family of shapes known capable of modeling wide variety of deformable objects, including the left ventricle (1, 19, 23). The parameters of the deformable shape modeling primitive are obtained through surface fitting when enough samples points of the surface are given. An implicit equation of the basic superquadrics can be written as:

$$\left( \left( \frac{x}{a_x} \right)^{2/\epsilon_2} + \left( \frac{y}{a_y} \right)^{2/\epsilon_2} \right)^{\epsilon_2/\epsilon_1} + \left( \frac{z}{a_z} \right)^{2/\epsilon_1} = 1. \quad (9)$$

where scale parameters  $a_x, a_y, a_z$  define the size of the superquadrics in the  $x, y$ , and  $z$  directions, respectively,  $\epsilon_1$  is the squareness parameter along the  $z$  axis and  $\epsilon_2$  is the squareness parameter in the  $x - y$  plane. We have extended the basic superquadric model to include

tapering and bending deformations (21) so that it would characterize the left ventricle shape better. The tapering deformation allows the model to capture the varying size of the cross sections and can be written as:

$$\begin{aligned} X &= (kz + 1)x \\ Y &= (kz + 1)y \\ Z &= z \end{aligned} \quad (10)$$

where  $k$  is a tapering constant and  $-\frac{1}{a_2} < k < \frac{1}{a_2}$ .

The estimation of tapering deformation can be incorporated into the fitting of superquadric modeling primitives since its linear nature would not complicate the fitting process. In general, the incorporation of bending deformation estimation to the model fitting is complicated because of its second order representation. This is why we choose to estimate bending deformation from long axis arc fitting and use the estimation result to unbend the given boundary points before the fitting of the superquadric surface modeling primitives. The fitting of the extracted left ventricle boundary to the surface modeling primitives has been implemented as nonlinear optimization. The objective function of the nonlinear optimization is expressed as the ‘‘inside-outside’’ function of the superquadrics summed over all given surface sample points. The ‘‘inside-outside’’ function is defined as:

$$f(x, y, z) = \left( \left( \frac{x}{a_x} \right)^{2/c_2} + \left( \frac{y}{a_y} \right)^{2/c_2} \right)^{c_1} + \left( \frac{z}{a_z} \right)^{2/c_1} \quad (11)$$

where, if  $f(x_0, y_0, z_0) = 1$ , then  $(x_0, y_0, z_0)$  is on the surface; if  $f(x_0, y_0, z_0) < 1$ , then  $(x_0, y_0, z_0)$  lies inside the surface; if  $f(x_0, y_0, z_0) > 1$ , then  $(x_0, y_0, z_0)$  lies outside the surface. The objective function for the optimization is defined as:

$$\text{Minimize: } \sum_{i=1}^n |f(x_i, y_i, z_i) - 1|^2 \quad (12)$$

where the summation is over all extracted surface points. With the inclusion of tapering deformation, the optimization is rewritten as:

$$\text{Minimize: } \sum_{i=1}^n |f(X_i, Y_i, Z_i) - 1|^2. \quad (13)$$

It is well known that the nonlinear optimizations are computationally intensive. We have, however, worked towards reducing the complexity of the optimization using a sequential fitting scheme (2).

#### 4.3 Feedforward and feedback algorithms

Sections 4.1 and 4.2 described, respectively, the algorithms for image segmentation and shape analysis.

It has been pointed out earlier that these two processes are traditionally implemented separately in existing surface modeling based image analysis approaches. We have also discussed how these two processes can benefit from each other if constructive interactions between them can be identified and positive influences can be enforced. We present here the algorithms to link these two processes through the design of the feedforward and feedback channels in this integrated approach.

The feedforward channel is composed of the steps needed to compute the confidence measures associated with the extracted boundary points. The confidence measure of a given boundary point is directly related to the neighborhood statistics derived from the original gray level image, and is used to represent the strength of a boundary point. The fitting of surface model weighted by such confidence measures generates a parameterized surface that will match well to the strong boundary sections but will be more flexible in weak boundary sections. The feedback channel consists of the steps needed to incorporate the surface model into the refinement of the segmentation. The goal of such incorporation is to use available shape information to guide the segmentation so that the effects of image distortion and reconstruction noise on image segmentation is reduced. Such a surface model based segmentation is capable of providing segmented regions corresponding well to both original image and the surface model.

*4.3.1 Confidence measure computation.* Two types of neighborhood statistics are used to measure the strength of a boundary point: local relative intensity, and local relative gradient. We define the overall average intensity of a segmented region as the averaged intensity of all points inside that region, and the local average intensity of a boundary points as the average intensity of all points within the intersection of a pre-defined neighborhood and the segmented region. In this research, we define a  $3 \times 3$  window centered on the given point as the neighborhood region, however, other types of neighborhood region can also be defined. The difference of these two average is used as one measure to characterize the strength of a boundary point; the small the difference, the stronger the boundary strength. The gradient of the a given boundary point is used as another measure to characterize the strength of a boundary point, since we expect that there is a sharp transition in intensity at these boundary points. In general, for a strong boundary point, its local average intensity is similar in value with the overall average intensity of the given region while the magnitude of its gradient is large. Therefore the strength of

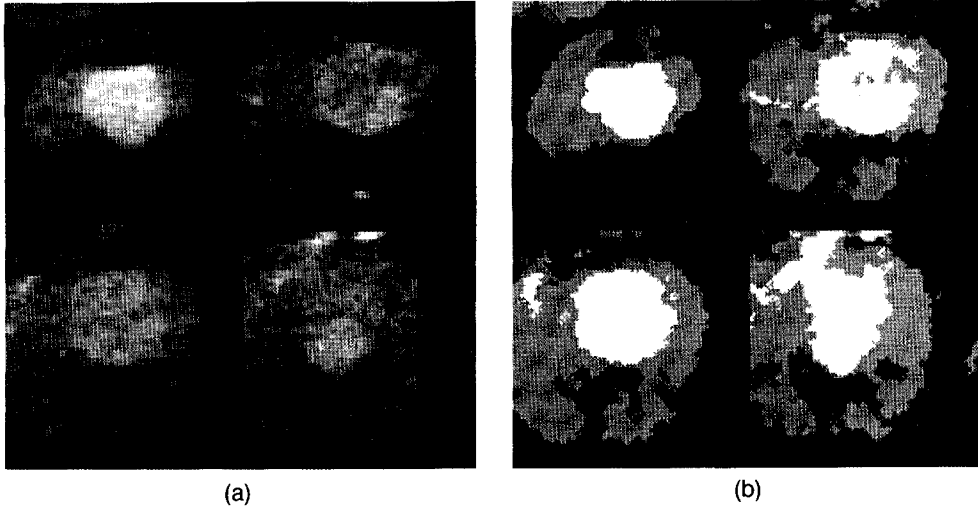


Fig. 3. (a) Initial segmentation results and (b) its comparison with the original data for a few typical cross sections.

boundary point, or the confidence measure, is proportional to the magnitude of the gradient and inversely proportional to the difference between its local average intensity and overall average intensity.

With the assumption of Gaussian intensity distribution for the clustered ROI, the local relative intensity  $C_I$  is defined as:

$$C_I = \exp\left(-\frac{|I_{\text{mean}} - I_{\text{local}}|}{\Delta I}\right) \quad (14)$$

where  $I_{\text{mean}}$  is the overall average intensity of the ROI,  $I_{\text{local}}$  is the local average intensity of pixels within the neighborhood of a given boundary point, and  $\Delta I$  is a

constant which is the standard deviation derived from distribution of the corresponding cluster. The local relative gradient  $C_G$  is defined as:

$$C_G = \frac{G_{\text{local}}}{G_{\text{max}}} \quad (15)$$

where  $G_{\text{local}}$  is the local gradient and  $G_{\text{max}}$  is the maximum gradient. The higher these two coefficients,  $C_I$  and  $C_G$ , the stronger is the boundary point. The weighted optimization of surface fitting then becomes:

$$\text{Minimize: } \sum_{i=1}^n C_I C_G |f(X_i, Y_i, Z_i) - 1|^2 \quad (16)$$

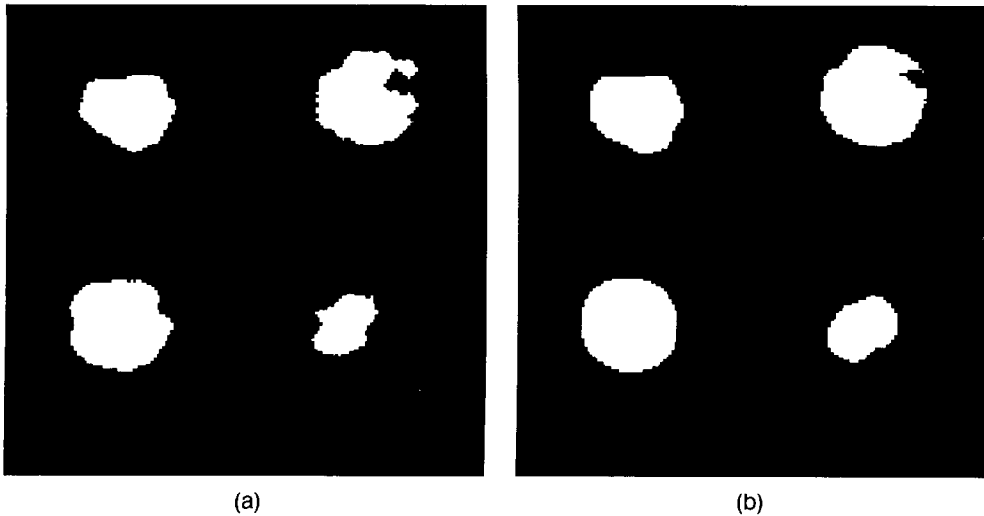


Fig. 4. (a) ROI identification result and (b) its comparison with the manually segmented result for the same cross sections presented in Fig. 3.

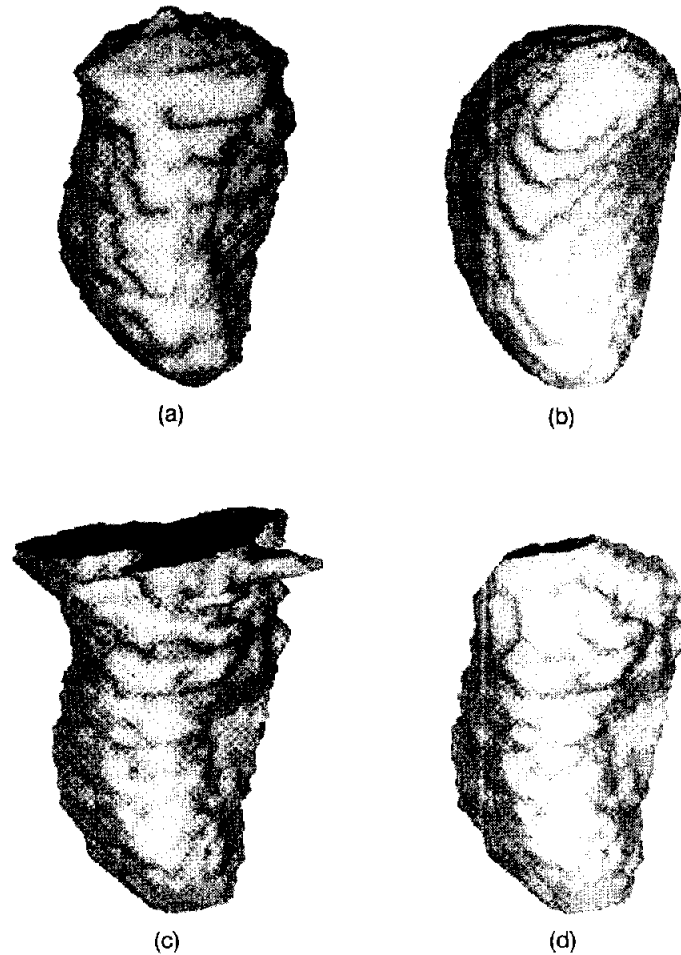


Fig. 5. Rendered volumes of the (a) manually segmented left ventricle chamber provided by Mayo Clinic, (b) the segmented region following the initial morphological operation, (c) the left ventricle chamber generated by predictive morphological operation, and (d) the parameterized surface created by fitting the extracted left ventricle to the superquadric surface model.

**4.3.2 Region masking and segmentation refinement.** The feedback channel serves as an effective way of incorporating the shape information into the process of segmentation refinement. In fact, we have utilized the shape information in the procedure of predictive morphological processing to identify the left ventricle region from the composite region that also contains left atrium and aorta. After the completion of the surface fitting, we have obtained a parameterized description of the left ventricle shape. The parameters of the fitted surface can then be used to guide the process of segmentation refinement. In particular, the scaling, tapering, and bending parameters of the fitted superquadrics can be used to construct a surface that can be projected into each cross section to create regions that would need necessary adjustment. The projected regions are to be compared with the regions obtained in the process of  $K$ -mean clustering to find out how the initial segmentation result conform with the shape

modeling primitives. No adjustment is necessary for those pixels which belong to consistent projected region and clustered region. After the comparison, two types of inconsistency are found among the pixels that need corresponding adjustment. The first type of inconsistently classified pixels are those clustered in the initial segmentation as the same class as the left ventricle but are not within the projected regions. They include the pixels corresponding to the left atrium and aorta that have been excluded from ROI in the process of predictive morphology. They also include pixels located outside of the fitted surface due to the smoothness constraints of the surface modeling primitives. The second type of inconsistently classified pixels are those clustered in the initial segmentation as not the same class as left ventricle but are within the projected regions. Such inconsistency is mainly due to the smoothness constraints of the surface modeling primitives.

To ensure the randomness of the pixel value ad-

justment, a stochastic updating scheme is implemented. We make use of a Gaussian distribution derived from the pixel value distributions of the initially segmented region-of-interest which includes the left ventricle and its adjacent segmented region. Suppose the pixel values in both regions can be represented as random variables with Gaussian densities. Then, the difference of these two random variables is another Gaussian and both mean and variance can be computed from the two given Gaussian distributions. For pixels with first type of inconsistency, since they are outside the projected region but inside the initial clustered region, we subtract from each pixel a random value generated from the distribution of difference we have derived so that their grey level are statistically closer to its adjacent cluster. For pixels with second types of inconsistency, since they are inside the projected region but outside the initial clustered region, we add to each pixel a random value generated from the same distribution so that their grey levels are statistically getting closer to the ROI. Such updated images are used as the input to the next iteration of the integrated approach.

## 5 RESULTS

Promising results have been obtained based on this integrated approach using one sequence of CT volumetric images. The results of image segmentation, ROI identification, and shape deformation analysis have all shown their consistency with both image data and a priori shape knowledge. Figure 3 shows the initial segmentation results of a few typical cross sections. In general, these regions include not only the left ventricle, but also the left atrium and aorta, as well as other types small regions that are generated by image acquisition noise. Figure 4 shows the result of ROI identification after a series of morphological operations for the same cross sections presented in Fig. 3. Notice that those small isolated regions have been eliminated and the regions corresponding to left atrium and aorta have been removed. The comparison of our ROI identification result with the manually segmented result shows that our morphological operation algorithms, in particular the predictive morphology algorithm designed to automatically remove the left atrium and aorta, are very successful. Figure 5 shows the 3D ren-

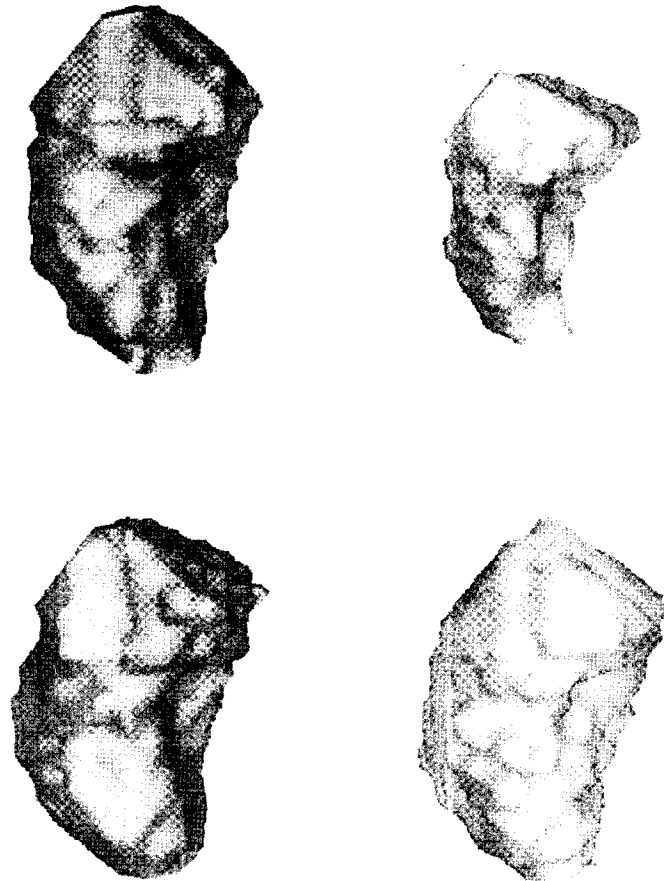


Fig. 6. Several rendered volumes of segmented left ventricle after the completion of ROI identification.

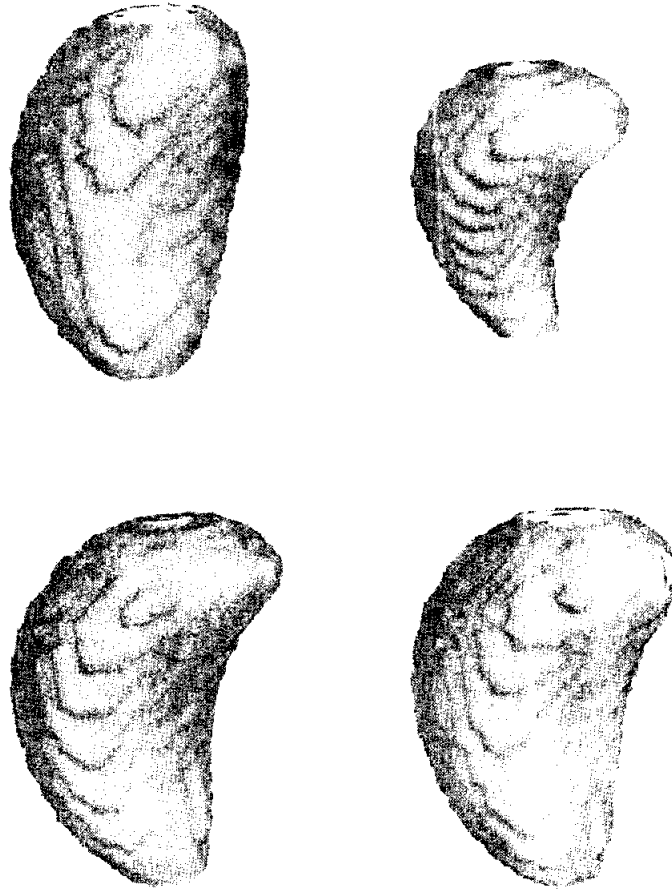


Fig. 7. Several rendered volumes of parameterized surface created by fitting the extracted left ventricle to the superquadric surface model.

derings of left ventricle obtained using different techniques. It clearly demonstrated that this integrated approach is capable of achieving very promising results beyond the manual operation and other semi-automatic segmentation algorithms since it provide not only accurately segmented volumes, but also the parameterized shapes that characterize the motion and deformation of the left ventricle. Figure 6 shows a few typical volumes of the segmented left ventricle and Fig. 7 shows their corresponding parameterized surfaces.

## 6 CONCLUSION

We have presented an integrated approach which unifies the image segmentation with the shape analysis. The application of this approach to the left ventricle motion analysis has shown that the traditionally separated image processing and image analysis processes can be integrated through the design of proper feedforward and feedback channels. Such integration of different image processing and image analysis is particularly suitable for applications when a priori information

of the object in the given image is known. For biomedical applications, this integrated approach can be very successful since we often seek to analyze structures in the images with known topological and morphological properties. Our success in left ventricle motion and deformation analysis based on the integrated approach has demonstrated the importance of using a priori knowledge in the surface modeling based image analysis tasks. The impact of this research will certainly reach beyond the specific application of integration to the left ventricle motion analysis. The methodology of the integration developed in this research can be applied to other types of shape structures and other imaging modalities.

The adaptive *K*-mean segmentation algorithm may also be extended to 4D to generate a coherent segmentation in the time domain using the temporal information of the given volumetric image data. Estimation algorithms for left ventricle local deformation will be developed to completely characterize the dynamics of the left ventricle. We will also investigate

different types of surface models and explore their applications to other biomedical image analysis problems.

*Acknowledgment*—This work was supported by NSF Grants IRI-89-08255, EEC 92-09615 and JSEP Grant N00014-90-J-1270. The authors wish to thank Dr. E. Hoffman of University of Iowa and Dr. W. Higgins of Penn State University for providing the CT image data, E. Ashton of University of Rochester for providing a preliminary version of the *K*-mean program.

## REFERENCES

- Chen, C.W.; Huang, T.S. Surface modeling in heart motion analysis. In: Silberman, M.J.; Tagare, H.D., eds. *Curves and Surfaces in Computer Vision and Graphics II*. vol. 1610. Boston, MA: SPIE; November 1991: 360–371.
- Chen, C.W.; Huang, T.S. Analysis of left ventricle global deformations based on dynamic CT data. In: *Proceedings international conference on pattern recognition*. The Hague, The Netherlands; August 1992.
- Widrow, B. The "rubber mask" technique—I and II. *Patt. Recogn.* 5:175–211; 1973.
- Yullie, A.L.; Cohen, D.S.; Hallinan, P.W. Feature extraction from faces using deformable templates. In: *Proceedings IEEE conference computer vision pattern recognition*. June 1989: 104–109.
- Grenander, U.; Chow, Y.; Keenan, D.M. *Hands: A pattern theoretic study of biological shapes*. New York: Springer-Verlag; 1991.
- Gritton, C.W.K.; Parrish, E.A., Jr., Boundary location from an initial plan: The bead chain algorithm. *IEEE Trans. Patt. Anal. Machine Intell.* 5:8–13; 1983.
- Cooper, D.B. Maximum likelihood estimation of Markov-process blob boundaries in noisy images. *IEEE Trans. Patt. Anal. Machine Intell.* 4:372–384; 1979.
- Kass, M.; Witkin, A.; Terzopoulos, D. Snakes: Active contour models. *Int. J. Comput. Vision* 1:321–331; 1988.
- Ritman, E.L. Fast computed tomography for quantitative cardiac analysis—state of the art and future perspectives. *Mayo Clinic Proc.* 65:1336–1349; 1990.
- Hoffman, E.A.; Ritman, E.L. Shape and dimensions of cardiac chambers: Importance of CT section thickness and orientation. *Radiology* 115:739–744; 1985.
- Higgins, W.E.; Chung, N.; Ritman, E.L. Extraction of left ventricle chamber from 3D CT images of the heart. *IEEE Trans. Med. Imaging* 9:384–395; 1990.
- Robb, R.A., ed. *Three-dimensional biomedical imaging*. Boca Raton, FL: CRC Press; 1985.
- Pappas, T. An adaptive clustering algorithm for image segmentation. *IEEE Trans. Signal Proc.* 40:901–914; 1992.
- Chang, M.M.; Tekalp, A.M.; Sezan, M.I. Bayesian segmentation of MR images using 3D Gibbsian priors. In: Rabbani, M.; Sezan, M.I.; Tekalp, A.M., eds. *Image and video processing*. vol. 1903. San Jose, CA: SPIE; February 1993.
- Giardina, C.R.; Dougherty, E.R. *Morphological methods in image and signal processing*. Englewood Cliffs, NJ: Prentice Hall, 1988.
- Higgins, W.E.; Hansen, M.W.; Sharp, W.L. Interactive relaxation labeling for 3D cardiac image analysis. In: Acharya, R.S.; Goldgof, D.B., eds. *Biomedical Image Processing and Biomedical Visualization*. vol. 1905. San Jose, CA: SPIE; February 1993.
- Luo, J.; Chen, C.W.; Parker, K.J.; Huang, T.S. 3D image segmentation via adaptive *K*-mean clustering and knowledge-based morphological operations. *IEEE Trans. Image Processing*. (in press).
- Chen, C.W.; Huang, T.S. Left ventricle motion analysis by hierarchical decomposition. In: *Proceedings International confer-*

ence acoustics, speech and signal processing. San Francisco, CA: III:273–276; March 1992.

- Terzopoulos, D.; Metaxas, D. Dynamic 3D models with local and global deformations: Deformable superquadrics. *IEEE Trans. Patt. Anal. Mach. Intell.* 703–714; July 1991.
- Potel, M.J.; MacKay, S.A.; Rubin, J.M.; Aisen, A.M.; Sayre, R.E. Three-dimensional left ventricular wall motion in man coordinate systems for representing wall movement direction. *Invest. Radiol.* 19:499–509; 1984.
- Chen, C.W. Left ventricle motion and shape modeling, analysis, and visualization from image sequences. PhD Thesis. University of Illinois at Urbana-Champaign, August 1992.
- Bookstein, K.G.F.; Buda, A. Mean tensor analysis of left ventricular wall motion. *Comput. Cardiol.* 513–516; 1984.
- Pentland, A. Perceptual organization and the representation of natural form. *Artif. Intell.* 293–331; 1986.

**About the Author**—CHANG WEN CHEN received his B.S. degree in electrical engineering from University of Science and Technology of China in 1983, M.S.E.E. degree from University of Southern California, Los Angeles in 1986, and Ph.D. degree in electrical engineering from the University of Illinois at Urbana-Champaign in 1992.

He was a Research Assistant in the Signal and Image Processing Institute, University of Southern California, Los Angeles in 1986. From January 1987 to July 1992, he was a Research Assistant at the Coordinated Science Laboratory and the Beckman Institute, University of Illinois at Urbana-Champaign. In the summers of 1989 and 1990, he was employed at the National Center for Supercomputing Applications, Champaign, Illinois, working with the Visualization Service and Development Group. In August 1992, he joined the faculty of the Department of Electrical Engineering, University of Rochester. His current research interests include biomedical image understanding, image sequence processing and analysis, image and video coding, digital signal processing, medical imaging, computer vision, computer graphics, scientific visualization, and artificial intelligence. He is a member of IEEE, SPIE, and Tau Beta Pi.

**About the Author**—JIEBO LUO received the B.S. and M.S. degrees in electrical engineering from the University of Science and Technology of China, Hefei, China in 1989 and 1992, respectively. In 1994, he received MS in electrical engineering from the University of Rochester.

He was a Research Assistant in the Information Processing Center, University of Science and Technology of China, Hefei, China from 1989 to 1992. He is now a Ph.D. candidate and a Research Assistant in the Department of Electrical Engineering, University of Rochester. His current research interests include image and video coding, wavelets and fractals, medical image analysis, image processing and pattern recognition. He is a student member of IEEE and SPIE.

**About the Author**—KEVIN J. PARKER received the B.S. degree in engineering science, summa cum laude, from the State University of New York at Buffalo in 1976. His graduate work in electrical engineering was done at the Massachusetts Institute of Technology, with M.S. and Ph.D. degrees received in 1978 and 1981.

From 1981 to 1985 he was an Assistant Professor of Electrical Engineering at the University of Rochester; currently he holds the title of Professor of Electrical Engineering and Radiology. Dr. Parker has received awards from the National Institute of General Medical Sciences (1979), the Lilly Teaching Endowment (1982), the IBM Supercomputing Competition (1989), and the World Federation of Ultrasound in Medicine and Biology (1991). He is a member of the IEEE Sonics and Ultrasonics Symposium Technical Committee and serves as reviewer and consultant for a number of journals and institutions. He is also a member of the IEEE, the Acoustical Society of America, and the American Institute of Ultrasound in Medicine.

Dr. Parker's research interests are in medical imaging, linear and nonlinear acoustics, and digital halftoning.

**About the Author**—THOMAS S. HUANG received the B.S. degree from National Taiwan University, Taipei, Taiwan, China, and the M.S. and Sc.D. degrees from the Massachusetts Institute of Technology (MIT), Cambridge, MA, all in electrical engineering.

He was on the Faculty of the Department of Electrical Engineering at MIT from 1963 to 1973, and on the Faculty of the School of Electrical Engineering and Director of its Laboratory for Information and Signal Processing at Purdue University, West Lafayette, IN, from 1973 to 1980. In 1980, he joined the University of Illinois, Urbana-Champaign, where he is now Professor of Electrical and Computer Engineering and Research Professor at the Coordinated Science Laboratory, and at the Beckman Institute. During his sabbatical leaves, he has worked at the MIT Lincoln Laboratory, the IBM T. J. Watson Research Center, and the Rheinisches Landes Museum, Bonn, Germany; he has also held Visiting Professor positions at the Swiss Institutes of Technology in Zurich and Lausanne, University

of Hannover, Hannover, Germany, and INRS—Telecommunications, University of Quebec, Montreal, Canada. He has served as a consultant to numerous industrial firms and government agencies, both in the United States and abroad. His professional interests lie in the broad area of information technology, especially the transmission and processing of multidimensional signals.

Dr. Huang has published 11 books and over 300 papers in network theory, digital filtering, image processing and computer vision. He is a Fellow of IEEE and the Optical Society of America, and has received a Guggenheim Fellowship (1971-72), an A. V. Humboldt Foundation Senior U.S. Scientist Award (1976-77) and a Fellowship from the Japan Association for the Promotion of Science (1986). He also received the IEEE Signal Processing Society's Technical Achievement Award in 1987 and the Society Award in 1991. He was named University Scholar by the University of Illinois in 1990. He was the founding editor and is currently an area editor of the international journal, *Computer Vision, Graphics, and Image Processing*, and editor of the Springer Series in Information Sciences, published by Springer-Verlag.